

Phonon and spin dynamics in BaVS₃ single crystals

Z. V. Popović, G. Mihály, István Kézsmárki, H. Berger, L. Forró, V. V. Moshchalkov

Angaben zur Veröffentlichung / Publication details:

Popović, Z. V., G. Mihály, István Kézsmárki, H. Berger, L. Forró, and V. V. Moshchalkov. 2002. "Phonon and spin dynamics in BaVS₃ single crystals." Physical Review B 65 (13): 132301. <https://doi.org/10.1103/physrevb.65.132301>.

Nutzungsbedingungen / Terms of use:

licgercopyright

Dieses Dokument wird unter folgenden Bedingungen zur Verfügung gestellt: / This document is made available under the following conditions:

Deutsches Urheberrecht

Weitere Informationen finden Sie unter: / For more information see:

<https://www.uni-augsburg.de/de/organisation/bibliothek/publizieren-zitieren-archivieren/publizieren>



Phonon and spin dynamics in BaVS₃ single crystalsZ. V. Popović,^{1,*} G. Mihály,² I. Kézsmárki,² H. Berger,³ L. Forró,³ and V. V. Moshchalkov¹¹Laboratorium voor Vaste-Stoffysica en Magnetisme, Katholieke Universiteit Leuven, Celestijnenlaan 200D, B-3001 Leuven, Belgium²Department of Physics, Technical University of Budapest, H-1111 Budapest, Hungary³Institut de Génie Atomique, Ecole Polytechnique Fédérale de Lausanne, CH-1015 Lausanne, Switzerland

(Received 14 September 2001; published 19 March 2002)

We have measured Raman spectra of barium vanadium sulfide (BaVS₃) single crystals in a broad temperature range (15 K–300 K). Three Raman active modes are found at about 193, 350, and 366 cm⁻¹. The assignment of the observed modes of BaVS₃ is carried out on the basis of the symmetry coordinate analysis. The mode at 350 cm⁻¹ shows a dramatic intensity increase and a line asymmetry by lowering the temperature below 30 K. We believe that this behavior is connected with the orbital and spin ordering in this compound.

DOI: 10.1103/PhysRevB.65.132301

PACS number(s): 78.30.Hv, 71.27.+a, 75.30.Mb, 71.45.Gm

I. INTRODUCTION

Barium vanadium sulfide (BaVS₃) belongs to the *h-ABX₃* (*h*=hexagonal) perovskites, materials, which exhibit interesting effects that are directly related to the quasi-one-dimensional features of their crystal structure. During the past several years low dimensional quantum spin systems such as the spin-Peierls, spin-ladder, and antiferromagnetic Heisenberg linear-chain systems have attracted much attention.¹ In spite of the chainlike crystal structure BaVS₃ is nearly isotropic from electrical point of view.²

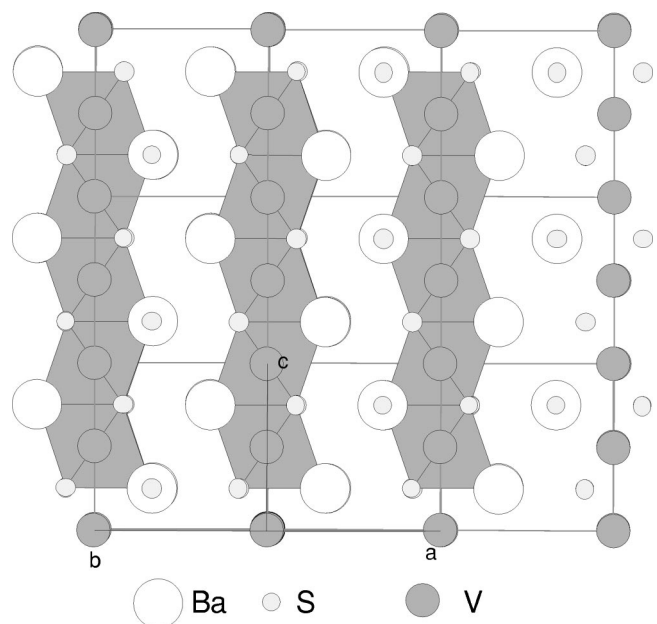
At ambient temperature BaVS₃ has a hexagonal crystal structure³ with space group *P6₃/mmc* and two formula units per unit cell (*Z*=2). Such crystalline structure assumes only one crystallographic position of vanadium atoms in V⁴⁺ valence state. Each vanadium atom is surrounded by six sulfur atoms, thus forming VS₆ octahedra. These octahedra are bound into face-sharing chains running along the *c* axis. The barium atoms are surrounded by 12 sulfur polyhedra.³ A schematic representation of the BaVS₃ crystal structure is given in Figs. 1 and 2.

BaVS₃ undergoes three phase transitions as a function of temperature. The first transition takes place at *T_S*=240 K and has been described as a crystallographic transition in which the crystal symmetry is reduced from hexagonal to orthorhombic⁴ with only a slight change in the resistivity.^{2,5} At this transition the dynamical distortion of the vanadium chains freezes and a static ordering of the vanadium sublattice appears. Above the transition the vanadium atoms are equidistant and form linear chains along the *c* axis, whereas below *T_S* they are still equidistant but the chains become zigzag. The size of the distortion gradually increases with decreasing temperature and saturates below about 20 K. The space group of the orthorhombic phase is *Cmc2₁*.⁶

The second transition, which takes place at *T_{MI}*≈70 K, is a sharp metal-insulator (MI) transition. At *T_{MI}* magnetic susceptibility shows a sharp peak and drops rapidly in the insulating state.^{2,5,7,8} Below this temperature resistivity increases abruptly and it drops by nine orders of magnitude down to about 20 K.^{2,5} The nature of the insulating phase is still controversial and has attracted considerable attention. From the X ray³ and the neutron-diffraction⁴ measurements

it was concluded that the lattice symmetry remained orthorhombic at all temperatures between 240 K and 5 K. Furthermore, the structural refinement based on neutron-diffraction powder data⁴ indicates that no major structural change takes place at the MI transition. There is only a small volume contraction of $\Delta V/V \approx 0.04\%$ (Ref. 5) and a jump in the size of the orthorhombic distortion.⁸

Both nuclear magnetic resonance or nuclear quadrupole resonance (NMR/NQR) (Ref. 9) and neutron-diffraction measurements⁴ have revealed that BaVS₃ has a nonmagnetic phase for *T*<*T_{MI}*. A huge and extraordinary asymmetric electric field gradient at the *V* sites appears at *T_X*≈30 K. This is the third phase transition that is also observable in macroscopic thermodynamic properties, such as the magnetic susceptibility and the magnetic anisotropy.² The above microscopic and macroscopic features were related to the development of a simultaneous orbital and spin ordering of the vanadium 3*d*¹ *t_{2g}* states.^{2,9} Evidences for antiferromagnetic type ordering were provided by neutron-scattering data.¹⁰

FIG. 1. Schematic representation of the BaVS₃ crystal structure.

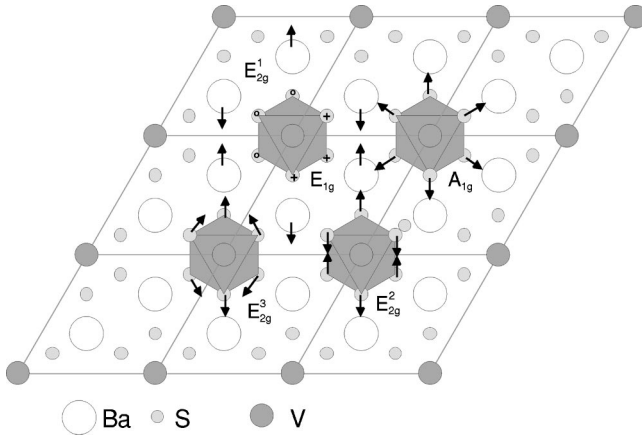


FIG. 2. Symmetry coordinates of the Raman-active modes of the hexagonal BaVS₃.

The resistivity measurements of the BaVS₃ single crystal under high pressure were described in Refs. 5,11,12. It has been shown¹¹ that the MI-transition temperature decreases with an increase of pressure and $T_X \rightarrow 0$ at 20 kbars. To the best of our knowledge, there is no data published about the vibrational properties of BaVS₃.

In order to clarify the role of phonons and spin excitations, we performed Raman scattering experiments on BaVS₃ single crystals. We assigned three vibrational modes by symmetry coordinate analysis. Besides this room-temperature study we also investigated the temperature dependence of the spectra. We found a dramatic intensity increase of the 350-cm⁻¹ mode, which is associated with the low-temperature spin and orbital ordering in the system.

II. EXPERIMENT

The present work was performed on single-crystal samples of BaVS₃ with dimensions typically about 1 × 0.3 × 0.3 mm³. The Raman spectra were measured in the back-scattering configuration using micro-Raman system with DILOR triple monochromator including liquid-nitrogen-cooled charge coupled device (CCD) detector. An Ar-ion laser was used as an excitation source. For low-temperature measurements we used Oxford Microstat He continuous flow cryostat with 0.5-mm thick window. Focusing of the laser beam was realized with a long-distance (10-mm focal length) microscope objective (magnification 50×). Overheating of the samples was observed with the laser power levels as low as 15 mW (1 mW at the sample).

III. RESULTS AND DISCUSSION

As it is already mentioned, the unit cell of BaVS₃ at room temperature is a primitive hexagonal with two formula units per unit cell. The site symmetries of Ba, V, and S atoms in the $P6_3/mmc(D_{6h}^4)$ space group are D_{3h}' , D_{3d} , and C_{2v}' , respectively. The factor group analysis (FGA) predicts¹³

$$(\text{Ba})(D_{3h}'), \quad \Gamma = A_{2u} + B_{1g} + E_{1u} + E_{2g},$$

$$(\text{V})(D_{3d}), \quad \Gamma = A_{2u} + B_{2u} + E_{1u} + E_{2u},$$

$$(\text{S})(C_{2v}'), \quad \Gamma = A_{1g} + A_{2g} + A_{2u} + B_{1g} + B_{1u} + B_{2u} \\ + E_{1g} + 2E_{1u} + 2E_{2g} + E_{2u}.$$

Summarizing these representations and subtracting the acoustic and the inactive modes, we obtained the irreducible representation of h -BaVS₃ vibrational modes,

$$\Gamma_{h\text{-BaVS}_3}^{\text{opt.}} = 1A_g(xx,yy,zz) + 1E_{1g}(xz,yz) \\ + 3E_{2g}(xx-yy,xy) + 3A_{2u}(\mathbf{E}\|\mathbf{z}) \\ + 4E_{1u}(\mathbf{E}\|\mathbf{x},\mathbf{E}\|\mathbf{y}). \quad (1)$$

According to this representation one can expect five Raman and seven infrared active modes. Note that the vibrations of the V atoms do not contribute in the scattering process (not Raman active).

Symmetry coordinates of all Raman active modes are shown in Fig. 2. According to the FGA, only one mode of E_{2g} symmetry (E_{2g}^1 mode, Fig. 2) originates from the Ba atom vibrations. This mode usually appears at the lowest frequency in the Raman spectra because of its heaviest mass. Other four Raman active modes originate from the vibrations of sulfur atoms. The total symmetric A_{1g} mode is a breathing mode of the VS₆ octahedra. This mode has the highest frequency in the Raman spectra of the h -ABX₃ perovskites.^{14–16} Since there is only one mode of this symmetry, its symmetry coordinate shown in Fig. 2, is actually the normal coordinate. The same is valid for the E_{1g} mode, which represents out-of-phase vibration of sulfur atoms along the c axis. The ion displacements of the A_{1g} and E_{2g} modes are in the c plane (Fig. 2). Since the $E_{2g}^{1,2,3}$ modes can couple (the same symmetry modes), the exact form of their normal coordinates can be obtained from the complete lattice-dynamical calculation. The symmetry coordinates of the E_{2g} modes given in Fig. 2 represent only the dominant form of these vibrations.

At $T = T_S = 240$ K the hexagonal structure transforms into orthorhombic with the unit-cell parameters $a_0 \approx a_h$, $b_0 \approx \sqrt{3}b_h$, $c_0 \approx c_h$, space group $Cmc2_1(C_{2v}^{12})$, and four formula units ($Z = 4$) comprising 20 atoms in all.⁶ The site symmetries of V, Ba, S₁, and S₂ atoms in (C_{2v}^{12}) space group are $(4a)$, $(4a)$, $(4a)$, and $(8b)$, respectively. The FGA yields

$$(\text{Ba}, \text{V}, \text{S}_1)(C_s^{yz}), \quad \Gamma = 2A_1 + A_2 + B_1 + 2B_2,$$

$$(\text{S}_2)(C_1), \quad \Gamma = 3A_1 + 3A_2 + 3B_1 + 3B_2.$$

Summarizing these representations and subtracting the acoustic ($A_1 + B_1 + B_2$) modes, we obtained the irreducible representations of the BaVS₃ vibrational modes of $Cmc2_1$ space group,

$$\Gamma_{r\text{-BaVS}_3}^{\text{opt.}} = 8A_1(xx,yy,zz,\mathbf{E}\|\mathbf{y}) + 6A_2(xy) \\ + 5B_1(xz,\mathbf{E}\|\mathbf{x}) + 8B_2(yz,\mathbf{E}\|\mathbf{y}). \quad (2)$$

Thus, 21 infrared and 27 Raman active modes are expected to show up in the BaVS₃ spectra, at temperatures below 240 K. Note that the optical modes of A_1 , B_1 , and B_2 symmetry are both infrared and Raman active, and the V atom vibrations take place in light scattering process.

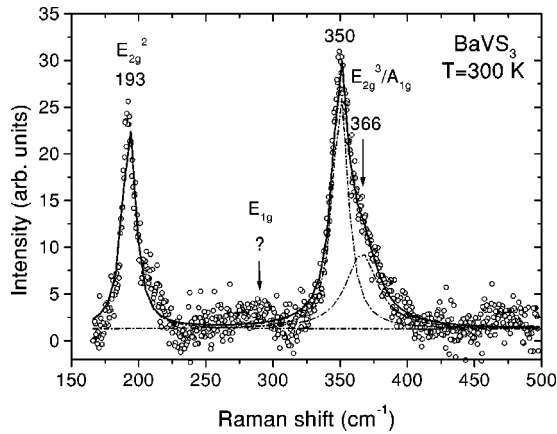


FIG. 3. Unpolarized room temperature Raman spectra (circles) of BaVS₃. Lorentzian profiles (dash-dot curves) are used to deconvolute the spectrum.

The unpolarized room-temperature Raman spectra of BaVS₃ is given in Fig. 3. Three modes at about 193, 350, and 366 cm⁻¹ are clearly observed. The highest frequency mode in the *h*-ABX₃ perovskites has the *A*_{1g} symmetry. Thus, we assigned the 366-cm⁻¹ mode as the *A*_{1g} mode of BaVS₃. According to the lattice-dynamical calculation of BaTiS₃ and BaNbS₃,¹⁷ the lowest frequency *E*_{2g}¹ mode, which represents vibrations of the Ba atoms, should appear at about 66 cm⁻¹. We do not observe this mode in our low-frequency Raman spectra due to a very weak intensity of this mode. Note that the Ba vibration mode is not registered in Ref. 17, also. We assigned the remaining two modes at about 193 and 350 cm⁻¹ as the *E*_{2g}² and *E*_{2g}³ modes. The 193-cm⁻¹ mode represents vibrations of the sulfur atoms that shear two sulfur triangles in the VS₆ octahedra. The analogous modes in BaTiS₃ and BaNbS₃ appear at 189 and 190-cm⁻¹, respectively.¹⁷ The 350-cm⁻¹ mode (*E*_{2g}³) originates from vibrations of the sulfur atoms which tend to deform VS₆ octahedra in a way shown in Fig. 2.

Finally, the *E*_{1g} mode corresponds to vibrations of the sulfur atoms along the *c* axis that tend to rotate the VS₆ octahedra, Fig. 2. The calculated frequency of this mode is 291 cm⁻¹.¹⁷ At this frequency we found a very weak structure, which can be *E*_{1g} mode (Fig. 3), similarly to the case of BaTiS₃ and BaNbS₃.¹⁷

According to the low-temperature Raman spectra, the orthorhombic distortion at about 240 K and the metal-insulator transition at *T*_{M_I} ~ 70 K have no observable influence on lattice dynamics of BaVS₃ [the appearance of new Raman modes, as predicted by FGA for orthorhombic phase, Eq. (2), is not observed]. At temperatures below *T*_X = 30 K, we found a dramatic change in the intensity of the 350 cm⁻¹ mode, as shown in Fig. 4.

There are several possible explanations for this feature. First we note that the 350-cm⁻¹ mode may be selected by the symmetry of the two low-lying vanadium orbitals² involved in the orbital ordering below *T*_X. Though in the first order the vanadium atom vibrations are not directly involved in the Raman-scattering process, we believe that the symme-

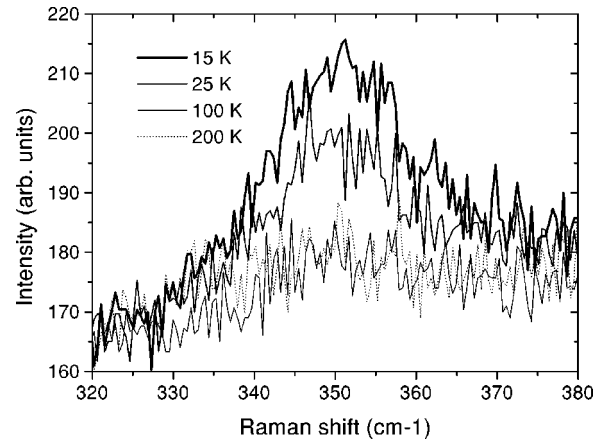


FIG. 4. The unpolarized Raman spectra of BaVS₃ at different temperatures in the 320–380 cm⁻¹ range. $\lambda_L = 514.5$ nm.

try breaking due to a static orbital order is associated to the unusual low-temperature enhancement of the corresponding Raman mode. Above *T*_X the dynamical fluctuations average out such an effect.

The second possibility is the electron-phonon coupling effect, observed in antiferromagnets.¹⁸ The model system in this respect is FeCl₂ with *T*_N = 23.5 K. In this compound the *E*_g-mode at 150 cm⁻¹ shows a strong line asymmetry above a peak energy and its broadening for *T* > *T*_N. For *T* < *T*_N the phonon line sharpens and a broad Gaussian-like excitation band is observed on the high-energy side, that shifts towards higher frequencies upon cooling down well below *T*_N. This band is due to the resonant electron-phonon interaction between the Fe²⁺ *d* level and the *E*_g phonon. Here, in the case of 350-cm⁻¹ mode in BaVS₃ we observed the similar feature as in FeCl₂ for *T* ≥ *T*_N (line asymmetry and a line broadening by increasing of the temperature). Due to the temperature limit of our experiment (15 K) we cannot give a definite proof for this scenario (an appearance of new broad band instead of an asymmetric tail of the 350-cm⁻¹ mode at temperatures well below *T*_X).

Another possibility is a spin-gap excitation superimposed with the 350-cm⁻¹ mode. By decreasing temperature the intensity of such a mode increases, together with the intensity increase of the associated continuum.¹⁹ The energy of 350-cm⁻¹ mode is very close to the 2Δ_S (≈ 500 K = 347 cm⁻¹) value, estimated from the NMR/NQR spin-gap data,⁹ which would suggest its magnetic origin. For the proper identification of such a magnetic mode very low-temperature dependent Raman spectra, as well as the spectra in magnetic field, are required.

Finally, the dramatic increase of the intensity of 350-cm⁻¹ mode can be due to its superposition with the two-magnon mode if the 3D spin ordering takes place in BaVS₃.²⁰ The energy of the two-magnon mode, associated with a top of the magnon brunch, is about 3J, where J is the exchange interaction. The 350-cm⁻¹ frequency gives exchange energy *J* = 168 K, very close to the value *J* = 163 K (Ref. 20) estimated from calorimetric study of BaVS₃.

In conclusion, the Raman spectra of the BaVS₃ single crystals are measured at room and low temperatures. We observed three Raman-active modes, two less than predicted by the factor-group analysis for hexagonal crystal structure of BaVS₃. The assignment of the BaVS₃ phonon modes is done on the basis of the symmetry coordinate analysis. The mode at about 350 cm⁻¹ shows a dramatic intensity increase by lowering the temperature below 30 K. This behavior is con-

nected with the simultaneous spin and orbital ordering in this compound.

ACKNOWLEDGMENTS

Z.V.P. acknowledges support from the Research Council of the K.U. Leuven and DWTC. The work at the K.U. Leuven is supported by the Belgian IUAP and Flemish FWO and GOA Programs.

*Permanent address: Institute of Physics, 11080 Belgrade P.O. Box 68, Yugoslavia.

¹E. Dagotto and T.M. Rice, *Science* **271**, 618 (1996).

²G. Mihály, I. Kézsmárki, F. Zamborszky, M. Miljak, K. Penc, P. Fazekas, H. Berger, and L. Forró, *Phys. Rev.* **61**, R7831 (2000).

³R.A. Gardner, M. Vlasse, and A. Wold, *Acta Crystallogr., Sect. B: Struct. Crystallogr. Cryst. Chem.* **B25**, 781 (1969).

⁴M. Ghedira, M. Anne, J. Chenavas, M. Marezio, and F. Sayetat, *J. Phys. C* **19**, 6489 (1986).

⁵T. Graf, D. Mandrus, J.M. Lawrance, J. D Thompson, and P. Canfield, *Phys. Rev. B* **51**, 2037 (1995).

⁶F. Sayetat, M. Ghedira, J. Chenavas, and M. Marezio, *J. Phys. C* **15**, 1627 (1982).

⁷M. Takano, H. Kosugi, N. Nakanishi, M. Shimada, T. Wada, and M. Koizumi, *J. Phys. Soc. Jpn.* **43**, 1101 (1977).

⁸M. Nakamura, A. Sekiyama, H. Namatame, A. Fujimori, H. Yoshihara, T. Ohtani, A. Misu, and M. Takano, *Phys. Rev. B* **49**, 16 191 (1994).

⁹H. Nakamura, H. Imai, and M. Shiga, *Phys. Rev. Lett.* **79**, 3779 (1997).

¹⁰H. Nakamura, T. Yamasaki, S. Giri, H. Imai, M. Shiga, K. Kojima, M. Nishi, K. Kakurai, and N. Metoki, *J. Phys. Soc. Jpn.*

69, 2763 (2000).

¹¹L. Forró, R. Gaál, H. Berger, P. Fazekas, K. Penc, I. Kézsmárki, and G. Mihály, *Phys. Rev. Lett.* **85**, 1938 (2000).

¹²I. Kézsmárki, Sz. Csonka, H. Berger, L. Forró, P. Fazekas, and G. Mihály, *Phys. Rev. B* **63**, 081106 (2001).

¹³D.L. Rousseau, R.P. Bauman, and S.P.S. Porto, *J. Raman Spectrosc.* **10**, 253, (1981).

¹⁴I.W. Jonstone, G.D. Jones, and D.J. Lockwood, *Solid State Commun.* **39**, 395 (1981).

¹⁵S. Jandl, M. Banville, Q.F. Xu, and A. Ait-Ouali, *Phys. Rev. B* **46**, 11 585 (1992).

¹⁶D.J. Lockwood, I.W. Johnstone, H.J. Labbe, and B. Briat, *J. Phys. C* **16**, 6451 (1983).

¹⁷M. Ishi and M. Saeki, *Phys. Status Solidi B* **170**, K49 (1992).

¹⁸D.J. Lockwood, in *Light Scattering in Solids III*, edited by M. Cardona and G. Güntherodt, Topics in Applied Physics Vol. 51 (Springer Verlag, Berlin, 1982), p. 59.

¹⁹M.J. Konstantinović, Z.V. Popović, M. Isobe, and Y. Ueda, *Phys. Rev. B* **61**, 15 185 (2000).

²⁰H. Imai, H. Wada, and M. Shiga, *J. Phys. Soc. Jpn.* **65**, 3460 (1996).